Coordination Chemistry Reviews, 128 (1993) 117–137

Kinetics and intermediates in the autoxidation of (cyclidene)iron(II) dioxygen carriers in a variety of solvent systems*

Alexandra Sauer-Masarwa[1], Lyndel D. Dickerson[2], Norman Herron[2] and Daryle H. Busch[1,2]

[1] *Department of Chemistry, University of Kansas, Lawrence, KS 66045 (USA)*

[2] *Department of Chemistry, The Ohio State University, Columbus, OH 43210 (USA)*

(Received 23 August 1992)

CONTENTS

ABSTRACT

The autoxidation of $[Fe^{II}(Me,Me,m\text{-}xyl)Cl]^+$ was studied in a variety of solvent systems, with the two extremes being aprotic acetonitrile containing the powerful axial ligand *N*-methylimidazole (MeCN/MIM) and protic methanol with the weak axial ligand chloride (MeOH/LiCl), and the results are compared with those from a previous investigation for the solvent system 3:1:1 acetone:pyridine:water (APW). The differences in the solvent systems are mainly manifested in the product distribution, whereas the rate law maintains its algebraic form and the previously proposed general mechanism of autoxidation (electron transfer operating in parallel with the dioxygen adduct equilibrium) requires only slight modifica-

* Dedicated to the memory of Professor John C. Bailar, Jr.

Correspondence to: D.H. Busch, Department of Chemistry, University of Kansas, Lawrence, KS 66045, USA.

0010-8545/93/$24.00

tion in order to account for the behavior of the full range of systems. Systems in which chloride serves as the axial ligand, yield only the product of the electron transfer step, $[Fe^{III}(Me,Me,m\text{-}xyl)Cl]^{2+}$, and its hydrolysis products, $[Fe^{III}(Me,Me,m\text{-}xyl)OH]^{2+}$, and $[\{Fe^{III}(Me,Me,m\text{-}xyl)\}_2O]^{4+}$. In contrast, systems in which the nitrogenous bases pyridine or 1-methylimidazole replace chloride as the axial ligand also produce a (peroxo)iron(III) species, in addition to $[Fe^{III}(Me,Me,m\text{-}xyl)B]^{3+}$, where the axial ligand depends on the medium. The formation of $Fe^{III}(Me,Me,m\text{-}xyl)OH]^{2+}$ and $[\{Fe^{III}(Me,Me,m\text{-}xyl)\}_2O]^{4+}$ depends, as expected, on the water content of the system. The effects of substituents, at constant bridging group and cavity size, on the autoxidation of $[Fe^{II}(R^3,R^2,m\text{-}xyl)Cl]^+$ with R^3 = Me, Ph and R^2 = Me, Bz in MeOH/LiCl are dramatic. Remarkably, the combined steric and/or electron-withdrawing effect of replacing methyl groups at both the R^2 and R^3 positions appears to be multiplicative rather than additive.

1. INTRODUCTION

Recently, we reported studies on the autoxidation of iron(II) cyclidene complexes having high relevance as the only available non-porphyrin models for the natural dioxygen carriers hemoglobin and myoglobin [1–4]. These substances share design features that forestall the bimolecular μ-peroxo bridge autoxidation mechanism of simpler systems [5]. In these model systems, dioxygen binding is forced to take place inside the protected cavity of the macrocycle by coordination of bulky axial bases, such as pyridine and *N*-methylimidazole, or highly solvated halide ions, at the single site available outside the cavity. Complexes of the cyclidene ligands enjoy the inertness that is characteristic of macrocyclic ligands, and equilibrium [6,7] and electrochemical studies [8] have established the conditions under which the axial ligand equilibria are saturated, providing further control over the solution compositions of these compounds. Those results are used in the design of the systems under study here.

Earlier studies of the autoxidation reactions of iron(II) cyclidenes having polymethylene bridging groups (R^1, structure **1**) ranging from trimethylene through hexamethylene have provided strong evidence for the mechanism defined by eqns. (1)–(6) [2–4]. The rate-determining step is assigned to an electron transfer between the iron(II) complex and unbound O_2 (eqn. (2)) and that reaction is in competition with the formation of the dioxygen adduct (eqn. (1)). This mechanism accords with that suggested for natural dioxygen carriers by Caughey and co-workers [9]. Thermodynamically, the one-electron autoxidation of these iron(II) complexes is unfavorable, and eqns. (3) and (4) show how the subsequent reaction of the primary product, superoxide, drives the reaction. For those lacunar cyclidene complexes with small cavities, these four equations suffice to describe the mechanism [1–4]. For those lacunar cyclidenes having larger cavities (pentamethylene and up), a second competition enters into the process, as solvent also binds inside the cavity, competing with O_2, and giving highly reactive intermediates that were first inferred, and then detected [2–4]. For these species, the dominant pathway involves eqns. (1) and (3)–(6).

All measurements reported here involve the iron cyclidene complexes of the general formula $[Fe^{II}(R^3,R^2,m\text{-}xyl)Cl]^+$ (**1**) with R^3 = Me, Ph and R^2 = Me, Bz, and

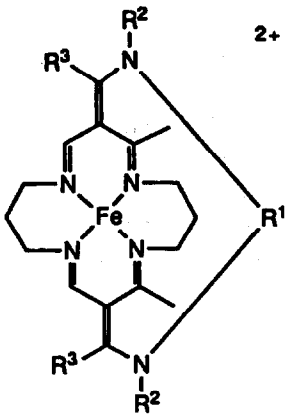

1

R^1 = m-xylylene. The dioxygen affinities of these *m*-xylylene-bridged complexes are closely similar to those having tetramethylene bridges; consequently, our working hypothesis will involve the mechanism of eqns. (1)–(4).

$$Fe^{II} + O_2 \rightleftharpoons Fe(O_2) \qquad K_{O_2} \tag{1}$$

$$Fe^{II} + O_2 \rightleftharpoons Fe^{III} + O_2^- \qquad k', k_2 \tag{2}$$

$$Fe^{II} + HO_2 \rightarrow Fe^{III} + HO_2^- \qquad k_3 \tag{3}$$

$$Fe^{III} + HO_2^- \rightleftharpoons Fe^{III}(HO_2^-) \tag{4}$$

$$Fe^{II} + S \rightleftharpoons Fe^{II}S \qquad K_S \tag{5}$$

$$Fe^{II}S + O_2 \rightarrow Fe^{III}S + O_2^- \qquad k_4 \tag{6}$$

It follows that data reduction has been in terms of the rate law given by eqn. (7).

$$\text{Rate} = \frac{k'[Fe^{II}][O_2]}{1 + K_{O_2}[O_2]} \tag{7}$$

A remarkable product of the autoxidation of $[Fe^{II}(Me,Me,m\text{-xyl})Cl]^+$ in the solvent system 3:1:1 acetone:pyridine:water (APW) is a (peroxo)iron(III) species, $[Fe^{III}L(O_2^{2-})]$, which can even be observed at ambient temperatures [1]. The detection and study of peroxo complexes is important because of their role in the mechanism of autoxidation (eqns. (3) and (4), above) and because they are novel biomimics. The O_2 adduct formed by the enzyme cyctochrome P450 is activated by receipt of an electron from a specific donor; at that point, the stoichiometry of the reactive intermediate corresponds to an iron(III) peroxo complex [10]. The ESR properties of $[Fe^{III}L(O_2^{2-})]$ are highly characteristic (low spin iron(III), $g = 2$ signal with an extremely low anisotropy) [1], and they closely resemble those of natural

systems (including Cytochrome P450) and their analogs [11]. Further, these species contrast with the first reported synthetic iron(III) peroxo complexes, which are high spin [12].

In this paper, we report the influence that changing the solvent and/or axial base have on the kinetics and product distribution in the autoxidation of iron(II) cyclidenes, mainly by comparing the earlier results with those from reactions in acetonitrile/1.5 M *N*-methylimidazole (MeCN/MIM) and in methanol/0.05 M LiCl (MeOH/LiCl). These media contrast strongly in their abilities to (1) support O_2 binding and (2) to promote autoxidation. The strong axial ligand in MeCN/MIM causes the iron(II) reactant to exist largely in the form of the dioxygen adduct, which we have previously shown inhibits autoxidation while its aprotic nature further disfavors the autoxidation processes by limiting the availability of essential protons for the driving reactions attributed to the reduction of superoxide (eqns. (3) and (4)). The contrasting MeOH/LiCl solvent system obviously provides a ready supply of protons and it also maintains a chloride axial ligand on the iron(II). As a result of the axial chloride ligand, no measurable concentrations of the dioxygen adduct are detected in the MeOH/LiCl system. The consequences of this strong contrast in solvent and ligation properties are revealing.

2. EXPERIMENTAL

2.1 Materials

Solvents and reagents were reagent grade or better. Solvents were distilled under nitrogen and degassed (freeze–pump–thaw method) prior to use. The synthetic route to the iron(II) [8] and iron(III) [13] complexes has previously been described.

2.2 Physical measurements

Fast atom bombardment (FAB) mass spectra were obtained on a VG ZAB HS mass spectrometer equipped with a xenon gun in a matrix of 3-nitrobenzyl alcohol (NBA). ESR were recorded on a Varian E-112 spectrometer operating in the X-band and the magnetic field was calibrated with external DPPH ($g = 2.0036$). Cyclic voltammetry experiments were performed using a Princeton Applied Research potentiostat (model 173) and universal programmer (model 175), the output being recorded directly to paper using a Houston Instruments 200 chart recorder. The working electrode was a 3 mm diameter vitreous carbon disk, sealed into Kel F (Bioanalytical Systems Inc.); the secondary/counter electrode was a platinum wire of large surface area and the reference electrode was a silver wire. All electrode potentials were measured vs. ferrocene, which was used as an internal standard. The supporting electrolyte was 0.05 M LiCl in the MeOH solvent and 0.05 or 0.1 M tetrabutylammonium tetrafluoroborate (TBAB) in acetonitrile. UV–Visible spectrophotometric

studies were conducted using a 1 cm gas-tight quartz cell, fitted with a gas inlet and a bubbling tube. Spectra were recorded on either a Varian 2300 spectrophotometer or a Hewlett Packard 8452 diode array spectrophotometer, with a 9000 (300) Hewlett Packard Chem Station. Both instruments incorporated flow-through temperature-regulated cell holders connected to a Neslab constant temperature circulation system, giving a temperature precision of ± 0.3°C. Oxygen/nitrogen gas mixtures were generated using Tylan FC-260 mass flow controllers. All inert atmosphere manipulations were performed in a nitrogen-filled Vacuum Atmospheres Corporation (VAC) glove box, equipped with a gas circulation and oxygen removal system, either a VAC MO40-1 or HE-493 dry train. Oxygen concentrations were maintained below 1 ppm.

Typical kinetic experiments began with filling a 1 cm gas-tight cell, fitted with a gas inlet and a bubbling tube, inside the glove box, with a solution of ca. 2×10^{-4} M cyclidene complex. In the case of CH_3CN/MIM, freshly prepared solutions were necessary because the complexes decomposed in that solvent system over several days, as was verified by lower absorbances and altered kinetic behavior. Solutions were saturated by initial bubbling for 120–180 s with the desired gas mixtures. Pseudo-first-order conditions of constant oxygen concentrations were achieved by occasionally bubbling more O_2 into the solution during the course of the experiment. Kinetic studies were performed with either of the spectrophotometers described above, and the kinetic parameters were evaluated using either the Hewlett Packard proprietary software or by using programs written in Basic for the Varian spectrophotometer by Dr. Naidong Ye of this group.

3. RESULTS

3.1 Autoxidation of [Fe^{II}(Me,Me,m-xyl)Cl]$^+$

3.1.1 Studies in acetonitrile/1.5 M N-methylimidazole (MeCN/MIM)

The difficulty of replacing the axial chloride ligand of [Fe^{II}(Me,Me,m-xyl)Cl]$^+$ with pyridine or *N*-methylimidazole in aprotic solvents of modest polarity has been studied and discussed at length [6–8]. Electrochemical and UV–Vis data reveal that chloride remains coordinated in anhydrous solutions [6–8]. An earlier study has shown that the dioxygen binding constant for a mixture of species having chloride and methylimidazole axial ligands changes with the ratio of those species, giving limiting values at the extreme equilibrium conditions [6]. In the present case, the high effective dioxygen binding constant observed for MeCN/MIM indicates that dioxygen facilitates replacement of the axial chloride, resulting in the dioxygen adduct with MIM as the axial base [6–8]. In addition, electrochemical measurements made in the absence of dioxygen at $T < -25$°C show that, at low temperatures, chloride can be at least partially replaced from the deoxy complex by MIM. The fact that MIM coordination is favored at lower temperature has been verified by monitoring the equilibrium between the two complexes, using their oxidative half-wave potentials. In contrast, those potentials were essentially unaffected by the addition of a nitroge-

nous base at room temperature. In summary, at room temperature and for a decade or two below, in degrees centigrade, the deoxy form of the complex is essentially all present as the chloride complex while the dioxygen complex exists as the methylimidazole derivative. In contrast, at lower temperatures the deoxy complex is a mixture of chloro and methylimidazole derivatives while the dioxygen adduct is all methylimidazole complex.

The product distribution and, therefore the spectral changes accompanying the autoxidation, depend on the oxygen pressure used, in close similarity to the previously investigated autoxidation reaction in 3:1:1 acetone:pyridine:water (APW) [1]. At low dioxygen pressures, the spectra show the formation of a product with maxima at 510, 630 and >820 nm, with one isosbestic point around 440 nm, and give essentially no indication of the presence of the dioxygen adduct during the reaction. At high dioxygen pressures and sufficiently low temperatures, one can observe the conversion of the initially formed dioxygen adduct (λ_{max} ca. 520, 600 sh nm) into products (λ_{max} ca. 650 nm). Figure 1 illustrates the UV–Vis spectral changes on autoxidation of solutions equilibrated with 760 torr of dioxygen at −20°C. The inset in this figure shows the first-order kinetic behavior of the reaction, as determined at 520 and 650 nm. The solid line in the latter is calculated and the symbols represent experimental points. The set of spectra show an isosbestic point around 570 nm, which is only well behaved at low temperatures (< −20°C), indicating decomposition of the reaction product at the higher temperatures, and therefore the rates obtained for formation of the initial autoxidation products are only reliable if measured at sufficiently low temperatures. As stated earlier [1–4], a useful advantage of these

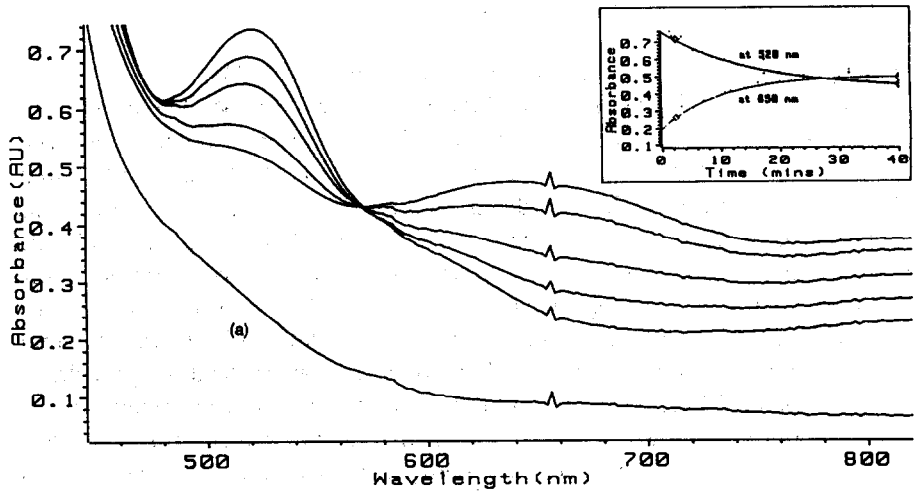

Fig. 1. Electronic spectral changes accompanying autoxidation of $[Fe^{II}(Me,Me,m\text{-}xyl)Cl]^+$ (2.9×10^{-4} M) in MeCN/MIM at −20°C, 760 torr. (a) Before oxygenation. Inset shows the kinetic traces at 520 and 650 nm and their first-order fits (solid lines).

systems is that they can be studied at temperatures where the formation of the primary oxidation products is the dominant process.

Table 1 summarizes the pseudo-first-order rate constants measured under a variety of conditions, and Fig. 2 displays the dioxygen dependence of the rates of product formation (for −16°C, measured at 650 nm). The reaction rate increases linearly with dioxygen pressure at low pressures but reaches a saturation value at high pressures, as was previously observed for autoxidation of the same compound in APW [1].

Figure 3 shows typical ESR spectral changes that have been observed during autoxidation. Solutions were oxygenated at temperatures in the range from −40 to

TABLE 1

Autoxidation rate constants for $[Fe^{II}(Me,Me,m\text{-xyl})Cl]^+$ in MeCN

Ligand	T (°C)	p_{O_2} (torr)	k_{obs}[a] (s^{-1})	Comments
MeCN/MIM (1.5 M)				
Me,Me,m-xyl	−16[b]	10	$1.4(1.5) \times 10^{-3}$	
		20	$2.5(3.4) \times 10^{-3}$	
		38	$3.0(4.3) \times 10^{-3}$	
		102	$4.2(—) \times 10^{-3}$	
		204	$3.9(—) \times 10^{-3}$	
		380	$3.8(2.1) \times 10^{-3}$	
	−10	760[c]	$5.0(2.1) \times 10^{-3}$	
	−15		$3.4(1.7) \times 10^{-3}$	
	−20		$1.7(1.1) \times 10^{-3}$	570 nm isosb. for ca. 20 min
	−23.0		$1.4(0.87) \times 10^{-3}$	572 nm isosb.
	−28.5		$6.5(6.0) \times 10^{-4}$	582 nm isosb.
	−33.7		$3.0(4.1) \times 10^{-4}$	586 nm isosb. for ca. 60 min
	−15	760[d]	3.29×10^{-3}	
			3.43×10^{-3}	0.14 M H_2O
			1.66×10^{-3}	0.7 M H_2O
			0.71×10^{-3}	2.6 M H_2O
MeCN/py (3:1)				
Me,Me,m-xyl	−12.5	760[e]	1.53×10^{-3}	
			1.57×10^{-3}	0.14 M H_2O
			1.56×10^{-3}	0.54 M H_2O
			0.99×10^{-3}	1.34 M H_2O
			0.68×10^{-3}	2.7 M H_2O

[a] At 650 nm, with values at 520 nm in parentheses, where available.
[b] $c_{Fe} = 2.3 \times 10^{-4}$ M.
[c] $c_{Fe} = 2.9 \times 10^{-4}$ M.
[d] $c_{Fe} = 2.2 \times 10^{-4}$ M.
[e] $c_{Fe} = 2.6 \times 10^{-4}$ M.

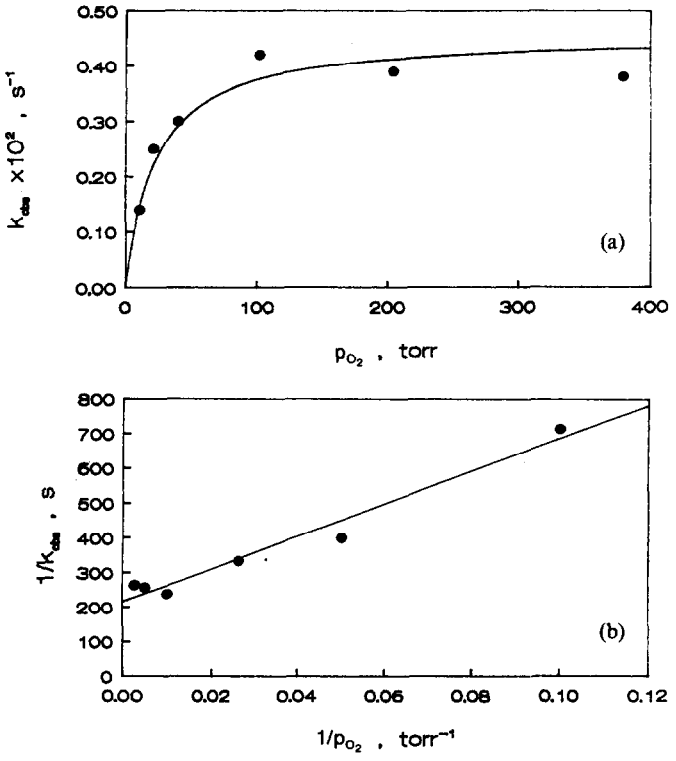

Fig. 2. Dioxygen partial pressure dependence of the rate of autoxidation and double reciprocal plot for $[Fe^{II}(Me,Me,m\text{-}xyl)Cl]^+$ in MeCN/MIM at −16°C.

−50°C and ESR spectra were measured at liquid nitrogen temperatures on solutions that are generally annealed at −20°C for various time periods. Several different paramagnetic products were observed. The main products are characterized by a quickly formed spectral pattern near $g = 2$, having highly distinctive spectral parameters. Initially, spectra assignable to a mixture of three or four low spin, six-coordinate, rhombic iron(III) complexes are observed. The resonances of two of the products*

* The other products in the $g = 2$ region display a larger spread of g values, indicative of "regular" axial ligands, possibly one nitrogen donor and one oxygen donor (MIM and OH^- being the most probable) or two oxygen donors [14(b),14(f),15]. These product signals are less intense compared with the pair of superimposed signals attributed to peroxo complexes and, further, because of those rather large overlapping signals only g values of 1.86, 1.95 and 2.43 can be identified. The signals at 1.86 and 2.43 apparently belong to one orthorhombic species since that set of signals can be independently produced by other routes ($g_1 = 1.86$, $g_2 = 2.25$ and $g_3 = 2.43$), and it shows no 1.95 signal. That spectrum is the only low spin pattern found in the reaction of the iron(III) cyclidene complex with H_2O_2 in aqueous MeCN/MIM, appearing without any noticeable evidence for the peroxide complex. The spectrum is also observed together with those for the two (peroxo)iron(III) derivatives when the autoxidation solutions from MeCN/MIM are concentrated by evaporating the MeCN. Moreover, that species is the only byproduct of the (peroxo)iron(III) when autoxidations are carried out in MeCN/MIM containing water (3:1, with ca. 3% H_2O).

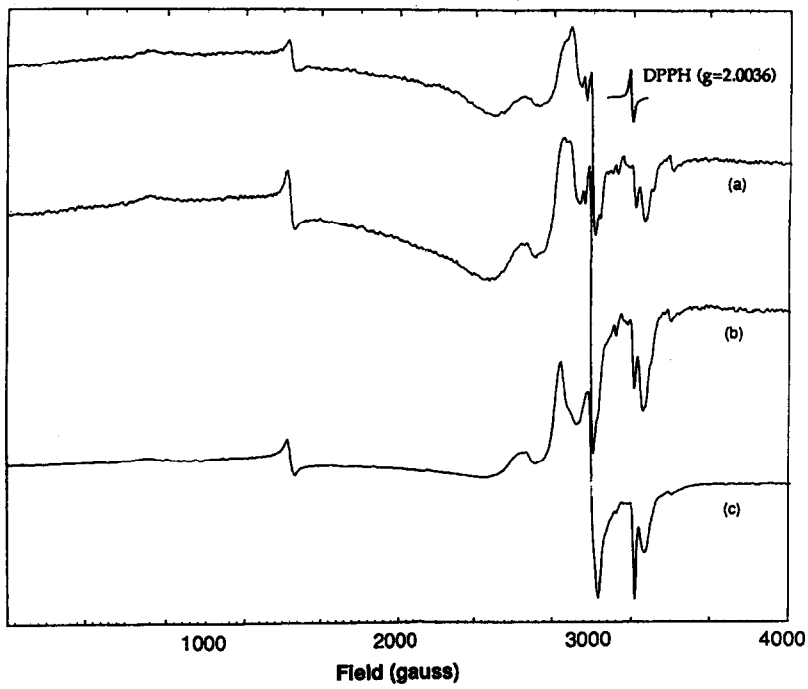

Fig. 3. ESR spectra of a frozen (−196°C) solution of $[Fe^{II}(Me,Me,m\text{-}xyl)Cl]^+$ (1.2×10^{-2} M) in MeCN/2.4 M MIM during autoxidation at 760 torr O_2, annealed at −20°C for (a) 2.5, (b) 7.5 (gain = 5×10^3) and (c) 27.5 min (gain = 1.25×10^3).

display an exceptionally weak orthorhombic anisotropy in close similarity to the pair of superimposed spectra reported earlier in the APW autoxidation studies [1]. The spectral features of one of them (g values of 1.93, 2.13, and 2.21) gradually disappear on longer annealing times (within ca. 20 min at 760 torr), while the resonances due to the second one (g values of 1.98, 2.11, and 2.24) increase during the same time period, allowing the distinction among the parameters*. That second set of signals persists even at room temperature. One of these products, or a mixture of the two, must be responsible for the electronic absorption maximum around 650 nm in the UV–Vis studies, that is associated with formation of the first autoxidation product. As a further connection between the UV–Vis kinetic studies and the ESR studies, at long times, solutions prepared for ESR studies also show this UV–Vis spectral feature and concentrated solutions prepared for UV–Vis autoxidation studies display an ESR spectrum corresponding to the same products.

Following the reasoning applied for the APW autoxidation products [1], the weakly anisotropic ESR signals are assigned to (peroxo)iron(III) species because of

* If the complex is autoxidized at lower dioxygen pressures (ca. 10 torr) a mixture of both signals is observed over time in the ESR studies; this explains the different product spectra in the UV–Vis investigations for low and high dioxygen pressures.

their close similarity to those found for natural systems [11], as well as to Tajima's model systems [14]. Interestingly, whereas peroxo product 2 formed in APW only on longer autoxidation timescales, that same product is apparently favored in MeCN/MIM.

In contrast to the APW system, the high-spin resonance pattern in the vicinity of $g = 6$ is not substantially present at any stage of reaction in the MeCN/MIM system. For comparison, the familiar, separately prepared high-spin iron(III) cyclidene complex [13] initially produces signals in the $g = 6$ region when dissolved in MeCN/MIM (a rather broad signal around $g = 8$)* and on dissolution in neat MeCN or MeCN/py (broad signal: ca. 7.4/4.8, signifying field parameters $E/D = 0.05$, corresponding to ca. 15% rhombicity** and indicating that Cl is still bound in the 5th axial position). Further, the response of the ESR spectrum to the addition of suitable reagents shows the spectral properties expected for the hydrolytic products of that complex. Following the addition of aqueous base to the iron(III) derivative in the MeCN/MIM, MeCN/py or MeCN systems, signals are observed at 6.4/5.8 (ca. 4% rhombicity**); these signals have previously been observed in other solvents and attributed to a six-coordinate complex with two weak axial ligands, e.g. OH, H_2O [1]. These signals also convert into a rather broad feature around $g = 8$ with excess base.

The fact that no observable amounts of high-spin products are formed during the autoxidation of the iron(II) cyclidene complex in MeCN/MIM provides further support for the conclusion that the initial autoxidation product is a peroxo complex***. Also, the eventual appearance, of the more strongly split $g = 2$ pattern supports the view that the strong ligand MIM remains bound at the axial position, and is eventually joined by a second axial ligand inside the cavity (perhaps OH^- formed by decomposition of peroxide), to produce another low spin product.

In summary, the reactants in solutions of $[Fe^{II}(Me,Me,m\text{-xyl})Cl]^+$ in acetonitrile/1.5 M methylimidazole contain the deoxy cation and, depending on dioxygen pressure, $[Fe(Me,Me,m\text{-xyl})(MIM)(O_2)]^{2+}$, in the vicinity of room temperature. At lower temperatures, some $[Fe^{II}(Me,Me,m\text{-xyl})(MIM)]^{2+}$ is also present. The autoxidation reaction in this system follows first-order kinetics for the complex

* The iron(III) complex is not stable in MeCN/MIM. After standing in solution, an ESR spectrum appears which shows a pattern similar to that produced by the autoxidation reaction of the iron(II) cyclidene complex, indicating autoreduction of the iron(III) in this system, with the resulting iron(II) complex undergoing autoxidation again. Precedence for this kind of behavior is reported for ferric porphyrins [16].

** Field parameters E/D and rhombicity are calculated based on the apparent splittings of the $g_\perp^{eff}$ resonances according to $\Delta g_{x,y} = 48E/D$ (or $g_{x,y}^{eff} = 6 \pm 24E/D$, where only one of the resonances could be determined with sufficient accuracy) and rhombicity $= (\Delta g_{x,y}/16) \times 100\%$ (see ref. 17).

*** In addition to the spectral patterns described above, especially on longer autoxidation timescales and/or at higher O_2 pressures, a weak, relatively narrow absorption is found near $g = 4.3$. Such spectral features have been attributed to rhombic, six-coordinate, high-spin iron(III), and, for porphyrins, assigned to a product arising from decomposition of the macrocycle [14(c),14(e)], a possibility that was considered for the iron(II) cyclidene APW system [1].

but obeys saturation kinetics with respect to O_2 partial pressure. The initial product of autoxidation of $[Fe^{II}(Me,Me,m\text{-xyl})Cl]^+$ in acetonitrile/MIM is a mixture of two peroxo complexes, and these eventually transform into more typical oxidation/hydrolysis products containing iron(III) and MIM plus, probably, OH. It is remarkable that no five-coordinate iron(III) is detected among the products.

3.1.2 Autoxidation products in acetonitrile with other axial bases

Autoxidation of $[Fe^{II}(Me,Me,m\text{-xyl})Cl]^+$ in MeCN or MeCN/LiCl yields products with λ_{max} of 530 and 650 sh nm (isosbestic point 435 nm) and λ_{max} of 530 and 664 sh nm (isosbestic point 490 nm), respectively, and corresponding ESR spectra featuring a broad signal in the $g = 6$ region (7.4, 4.8), and minor signals at $g = 4.3$ and $g = 2$ (1.98, 2.15, axial pattern). Titration of the iron(III) complex with OH^- converts the initial high-spin chloride complex (615 nm, $g = 7.4, 4.8$), via an intermediate with different spectra (e.g. 540 and 660 nm, depending on the extent of the change), into a high-spin hydroxo or aqua complex (λ_{max} of 500 and 650 sh nm, $g = 6.4, 5.8$), leading to the conclusion that a mixture of these two complexes is produced during autoxidation in those solvents. More of the chloride product is formed in the system with added LiCl, and that is responsible for the difference in isosbestic points and slight difference in spectral appearance.

Autoxidaton in 3:1 MeCN/py, in the presence of a small amount of water (max. 2.5 M), yields mainly the high-spin iron(III) OH/H_2O complex, as verified by ESR and UV–Vis spectroscopy (λ_{max} of 500, 650 sh nm; $g = 6.4, 5.8$), whereas the main product in MeCN/py (3:1) in the absence of added water is a high-spin iron(III) complex featuring a rather broad signal around $g = 8$ and corresponding UV–Vis maxima of ca. 520–530 and 670–680 (isosbestic point around 446 nm); the ESR spectrum of the latter indicates a rather large deviation from tetragonal symmetry with about 25% rhombicity (see footnote**, p. 126). The source of this signal is not obvious because most of the iron(III) in this solvent is coordinated to chloride and displays broad ESR signals at $g = 7.4, 4.8$. A signal around $g = 8$ can also be produced by adding larger amounts of OH^- to the iron(III) cyclidene complex in MeCN or by dissolving the iron(III) derivative in MeCN/MIM. On the other hand, the source of this broad $g = 8$ signal can be converted into the OH/H_2O complex ($g = 6.4, 5.8$) simply by the addition of slight amounts of water to acetonitrile/nitrogenous base systems.

In summary, the products of the autoxidation reactions in the solvent systems described in this section (MeCN, MeCN/LiCl, MeCN/py, MeCN/py/H_2O) are predominantly high-spin iron(III) species, with no indication of the characteristic (peroxo)iron(III) products, which had been observed in APW and in MeCN/MIM*.

* An exception to this behavior has been reported earlier [1]; an axial $g = 2$ signal of low anisotropy (2.16, 1.97) is the main product of the autoxidation in a carefully dried MeCN/py system.

3.1.3 Studies in methanol/LiCl

In the solvent methanol, at constant ionic strength and with the coordination of chloride as the axial ligand assured by the presence of excess LiCl (0.05 M), rapid autoxidation takes place even at temperatures as low as −50°C. Further, no measurable amount of dioxygen adduct is formed initially even at low temperatures. UV–Vis spectral data show the formation of a product with λ_{max} of 505 and 650 sh nm and an isosbestic point at ca. 410 nm (Fig. 4).

In Table 2, the observed rate constants are reported for a variety of conditions. Under pseudo-first-order conditions, the dioxygen dependence of the rate constants again obeys the saturation law (Fig. 5(a)). The rate is further dependent on base concentration, as was observed for the APW system [1], with the autoxidation rate increasing with the concentration of added base (Table 2 and Fig. 6). Pseudo-pH values are calculated, assuming a similarity between MeOH (pK = 16.7) [18] and H_2O (pK = 14) and using the measured starting pH (ca. 7, without added base) of the solvent system. This pH effect also manifests itself in the kinetic behavior of the compound in solvent dried by different methods. For this reason, solvent of corresponding history must be used in making comparisons.

ESR experiments show only one paramagnetic product from autoxidation of $[Fe^{II}Me,Me,m\text{-xyl})Cl]^+$ in the MeOH/LiCl system, the familiar high-spin Fe(III) complex with g values of 6.4/5.8 sh. Comparison of the characteristics of the autoxidation product in the methanol system with the chemically or electrochemically oxidized Fe(III) cyclidene complex confirms its identity as $[Fe^{III}LOH]^{2+}$. The reversible acid–base titration of (cyclidene)iron(III) shows three distinct derivatives, which have been characterized by UV–Vis, ESR, cyclic voltametry and mass spectroscopy, and

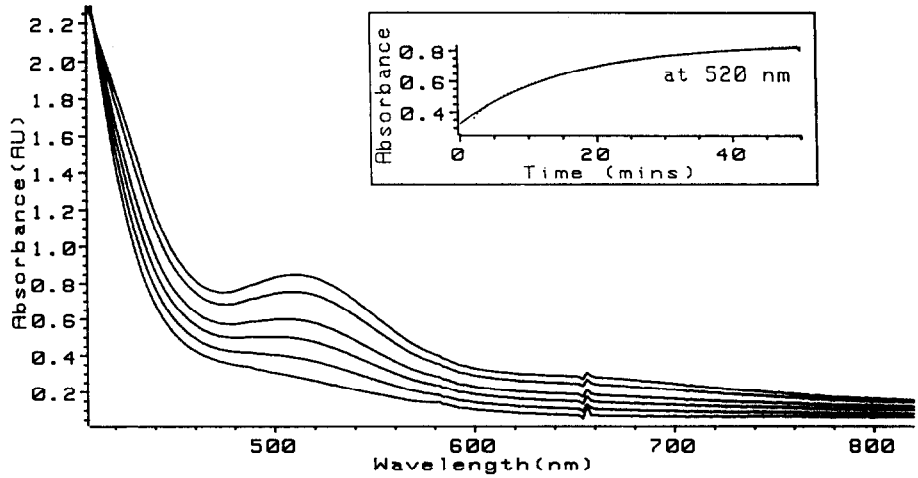

Fig. 4. Electronic spectral changes accompanying autoxidation of $[Fe^{II}(Me,Me,m\text{-xyl})Cl]^+$ in MeOH/LiCl (0.05 M) at −30°C, 2.5 torr O_2. Inset shows the kinetic trace at 520 nm and the first-order fit (solid line).

TABLE 2

Comparison of autoxidation rate constants for substituted iron(II) cyclidenes (R^1 = m-xyl) in MeOH/LiCl (0.05 M)

Ligand	T (°C)	p_{O_2} (torr)	k_{obs}[a] (s^{-1})	Comments
Me,Me,m-xyl	−30	19	1.5×10^{-3}	Solv. dried over Mg/I_2
		38	1.8×10^{-3}	
		100	3.5×10^{-3}	
		200	6.4×10^{-3}	
	−29.5	2.53	1.06×10^{-3}	Solv. dried over CaH_2
		6.33	2.37×10^{-3}	
		12.67	3.95×10^{-3}	
		25.33	7.67×10^{-3}	
		51.0	1.16×10^{-2}	
		102.0	1.76×10^{-2}	
		380.0	3.70×10^{-2}	
	−9.5	25.3	7.7×10^{-3}	[BuONa] = 0
		25.3	9.5×10^{-3}	[BuONa] = 5×10^{-5}
		25.3	9.8×10^{-3}	[BuONa] = 1.3×10^{-4}
		25.3	1.7×10^{-2}	[BuONa] = 2.5×10^{-4}
		25.3	3.0×10^{-2}	[BuONa] = 5×10^{-4}
	−25	0.9	1.83×10^{-4}	
		1.4	3.84×10^{-4}	
		1.9	4.57×10^{-3}	
		5.9	1.20×10^{-3}	
		13.0	1.89×10^{-3}	
		27.3	2.48×10^{-3}	
Me,Bz,m-xyl	−25	5.9	1.29×10^{-4}	
		38	4.95×10^{-4}	
		102	1.04×10^{-3}	
		238	1.74×10^{-3}	
		329	1.65×10^{-3}	
		746	2.12×10^{-3}	
Ph,Me,m-xyl	−25	99	2.86×10^{-4}	
		199	5.82×10^{-4}	
		298	7.32×10^{-4}	
		397	1.05×10^{-3}	
		497	1.16×10^{-3}	
		596	1.26×10^{-3}	
		745	1.32×10^{-3}	
Ph,Bz,m-xyl	+20	159	1.91×10^{-4}	
		239	2.33×10^{-4}	
		329	2.81×10^{-4}	
		529	3.75×10^{-4}	
		743	4.00×10^{-4}	

[a]Average for both 510–520 and 620–650 nm; closely similar behavior was observed in both wavelength ranges.

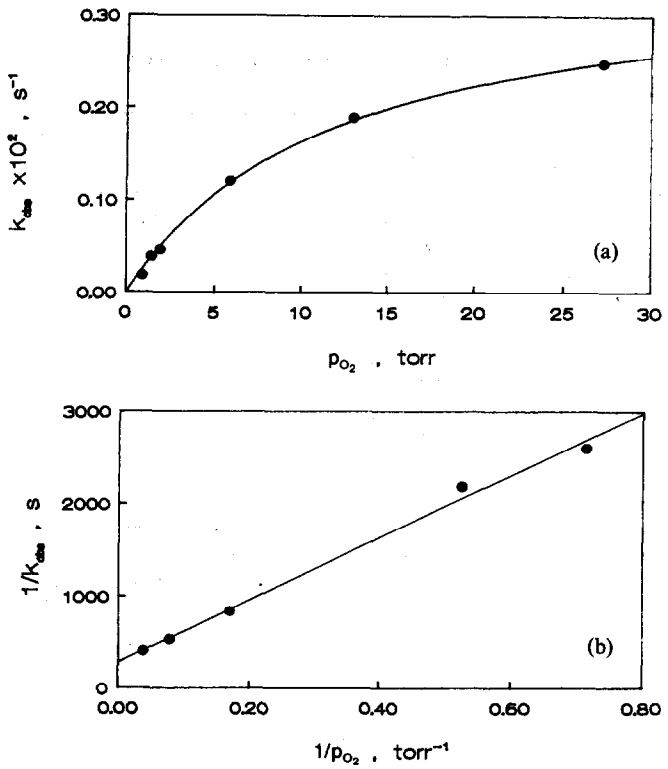

Fig. 5. Dioxygen partial pressure dependence of the rate of autoxidation and double reciprocal plot for $[Fe^{II}(Me,Me,m\text{-}xyl)Cl]^+$ in MeOH/LiCl at −25°C.

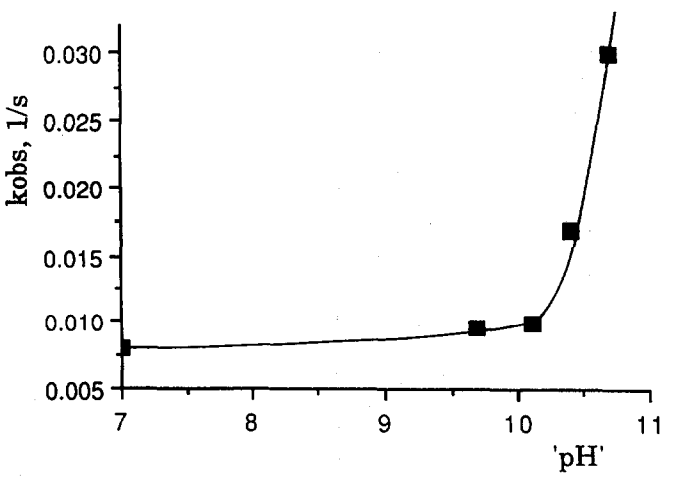

Fig. 6. Base dependence (addition of *t*-BuONa) on the rates of autoxidation of $[Fe^{II}(Me,Me,m\text{-}xyl)Cl]^+$ in MeOH/LiCl at −10°C, 25.3 torr O_2.

TABLE 3
Characteristics of iron(III) species in MeOH/LiCl

Conditions:	$Fe^{III}LCl$ Neutral	$Fe^{III}LOH$ +1 eq. base	$LFe^{III}—O—Fe^{III}L$ >1 eq. base
UV–Vis	610 nm	505, 650 sh nm	515 nm
$E_{1/2}$ vs. Fc	0.40	0.68 (irrev.)	0.98 (irrev.)
ESR	$g = 7.4, 4.8$	$g = 6.4, 5.8$	g around 8
Mass-spec.	552 m/z	533 m/z	1046 m/z

Table 3 summarizes the relevant data. The dissolution of Fe(III) in MeOH/LiCl alone leads to a mixture of $[Fe^{III}LCl]^{2+}$ and $[Fe^{III}LOH]^{2+}$. Mass spectrometry of the solid Fe(III) product that is obtained from solutions containing excess base shows peaks identifying the μ-oxo-dimer, the hydroxo and the chloro complex (according to m/z and the isotope distribution), confirming that these are distinct species existing during the titration of the iron(III) cyclidene with OH^-. A one-to-one accounting of the properties tempts us to assign the $g = 8$ ESR pattern to the μ-oxo complex* [19]. According to these results, the autoxidation product is $[Fe^{III}LOH]^{2+}$ and formation of this species requires 1 equivalent of base. This, in turn, indicates that the reaction medium increases in basicity during the autoxidation reaction, as expected on the basis of the mechanism of eqns. (1)–(4).

In summary, saturation of the equilibrium for binding of the axial chloride ligand is assured by working in 0.05 M LiCl. Under these conditions, no evidence has been found for dioxygen binding, even at low temperatures, indicating that the chloro complex has a very low dioxygen affinity. Autoxidation proceeds rapidly, displaying the usual behavior; simple first order in iron(II) complex and saturation kinetics with respect to dioxygen partial pressure. The only product formed during autoxidation at low temperatures is the high-spin five-coordinate hydroxy complex $[Fe^{III}(Me,Me,m\text{-}xyl)OH]^{2+}$.

4. DISCUSSION

The autoxidation behavior of $[Fe^{II}(Me,Me,m\text{-}xyl)Cl]^{+}$ displays strikingly similar kinetic profiles in a variety of solvents ranging from the aprotic solvent acetonitrile having the strong axial base *N*-methylimidazole as a co-solute, to the protic medium MeOH/LiCl, in which the axial ligand is the chloride ion. In all cases, the

* There are two problems with assigning the very broad high spin signal around $g = 8$ to a μ-oxo-dimer: (1) such species are generally antiferromagnetically coupled and therefore mostly ESR silent (although spectra have been reported in a few cases) [19]; (2) the similar signals found for Fe(III) cyclidenes in MeCN/MIM and upon autoxidation of the same compound in MeCN/py should then be assigned to such species. The rationale for the latter is that very small amounts of water stabilize the μ-oxo-dimer with respect to the hydroxo complex.

reaction is simple first order in iron(II) while obeying saturation kinetics with respect to the partial pressure of dioxygen. In both respects, the kinetics are in agreement with the previously reported mechanism given in eqns. (1)–(4), above. However, the saturation behavior in all solvent systems is somewhat surprising since the dioxygen affinities of the dominant species vary greatly over the range of solvents. In the presence of nitrogen bases as axial ligands, the formation of the dioxygen adduct (eqn. (1)) represents a competitive equilibrium and provides a convincing rationale for the saturation behavior. In contrast, no O_2 complex can be detected in the MeOH/LiCl medium so that the saturation behavior is not so easily explained. Further, the low-temperature reaction products differ with solvent/axial ligand system: in the most potent system, CH_3CN/MIM, only low-spin iron(III) is formed and the predominant products are peroxo species, but in the system with least O_2 affinity, the simple high-spin five-coordinate hydroxy complex is the sole product. Solvent systems having intermediate properties (APW) give mixtures of the two extreme behaviors.

4.1 Initial autoxidation products

Table 4 gives a summary of the main products of the autoxidation of $[Fe^{II}(Me,Me,m\text{-xyl})Cl]^+$ for each of the solvent systems studied. The generalization can be made that the dioxygen adduct and the (peroxo)iron(III) complex seem to require similar conditions in order to form. Solvent/axial base systems which do not support the presence of the dioxygen adduct also do not produce the peroxo species in the course of autoxidation. Neither the dioxygen adduct nor the peroxo complex is formed in measurable amounts under conditions where Cl is a major axial ligand. Reviewing the observations, autoxidation yields a peroxo complex $Fe^{III}(HO_2^-)$ in APW and MeCN/MIM, but it fails to do so in MeOH/LiCl, MeCN or MeCN/py. (In very dry MeCN/py, a similar peroxo species appears to form, but it displays a unique axial ESR signal with closely spaced g values of 2.16 and 1.97.) In the latter

TABLE 4
Main products of autoxidation of $[Fe^{II}(Me,Me,m\text{-xyl})Cl]^+$

Solvent system	High-spin products			Low-spin products	
	$LFe^{III}Cl$	$LFe^{III}OH$	$LFe^{III}—O—Fe^{III}L$	$LFe^{III}(X)(B)$	$LFe^{III}(O_2^{2-})(B)$
MeOH/LiCl		×			
MeCN/(LiCl)	×	×			
MeCN/py			×		
MeCN/py/H_2O		×			
MeCN/MIM				×	×
APW [1]		×			×

solvent systems, the products of the autoxidation reaction are high-spin iron(III) species, which can be produced by simple electron transfer from the iron(II)cyclidene, with the axial base depending on the medium. The appearance of the low-spin peroxo complexes in APW and MeCN/MIM suggests that an axial base of sufficient strength to yield low spin iron(III) is necessary in order for a stable peroxo complex to form.

4.2 Mechanistic implications

As stated above, kinetic data obtained for the solvent system MeOH/LiCl show saturation kinetics. However, in this case, data analysis (Figs. 2(b) and 5(b)) yields kinetic parameters which cannot be ascribed to the simple competitive equilibrium model in which the formation of a dioxygen adduct competes with outer sphere autoxidation. For the MeOH/LiCl system, the K_{O_2} values calculated from eqn. (7) far exceed the actual dioxygen affinities of the iron(II) complexes under these conditions. Further, the equilibrium constants for O_2 binding that are calculated from kinetic data for the APW system are also too large in comparison to those obtained for the MeCN/MIM system; the APW numbers should be substantially lower than those for MeCN/MIM. Only the value for MeCN/MIM appears to conform to the simple model. The expected dioxygen affinities for the MeOH/LiCl systems are lower than those in any of the other solvent systems treated here [6]. For example, the value of K_{O_2} calculated from eqn. (7) for MeOH/LiCl at $-30°C$ amounts to between 0.02 and 0.08 $torr^{-1}$, much too high compared with the extrapolated K_{O_2} value in APW (0.02 $torr^{-1}$ at $-20°C$) [6,8]. There are no available K_{O_2} data for $[Fe^{II}(Me,Me,m\text{-}xyl)Cl]^+$ in MeOH solutions because the complex autoxidizes, even at low temperatures in that medium. Even for the remarkably unreactive $[Fe^{II}(Ph,Bz,m\text{-}xyl)Cl]^+$ (vide infra) the K_{O_2} value was too small to be measurable, even at temperatures as low as $-40°C$.

These results indicate that, in these systems, follow-up reaction (3) also has to be taken into account mathematically, which then yields the following rate law (steady-state treatment of superoxide concentration).

$$-\frac{d[Fe^{II}]}{dt} = \frac{2[k'k_3/(k_3-k_2)][Fe^{II}]^2[O_2]}{\{1-[k_2K_{O_2}[O_2]/(k_3-k_2)]\}[Fe^{II}]+[k_2/(k_3-k_2)][Fe^{II}_0]}$$

According to the experimental rate law, the last term in the denominator vanishes, resulting in the simplified rate law:

$$-\frac{d[Fe^{II}]}{dt} = \frac{2k'k_3[Fe^{II}][O_2]}{(k_3-k_2)-k_2K_{O_2}[O_2]} \tag{8}$$

Because of the form of the rate law and the number of constants, it is convenient to restate it in a familiar form analogous to the Michaelis–Menton law, which, again, represents a competitive equilibrium. Thus the two parameters extractable from the law are k_a and K_b, in analogy to the well known k_{cat} and K_m. Parameters k_a and

K_b are reported in Table 5.

$$-\frac{d[Fe^{II}]}{dt} = \frac{k_a[Fe^{II}][O_2]}{1 + K_b[O_2]} \quad (9)$$

where $k_a = 2k'k_3/(k_3 - k_2)$ and $K_b = -k_2K_{O_2}/(k_3 - k_2)$, with k_a replacing the previously defined rate constant k' and K_b, K_{O_2}.

In summary, it can be stated that the systems with strong axial ligands (MeCN/MIM and, possibly, APW) can be modeled well by a mechanism based on simple electron transfer between the iron(II) complex and dioxygen in competition with dioxygen binding, whereas follow-up reactions have to be taken into account to successfully model the autoxidation in MeOH/LiCl and similar solvent systems within which only weak axial ligands are present.

4.3 Effects of substituents on autoxidation of [Fe(R², R³,m-xyl)Cl]⁺

The influence of the substituents R^2 and R^3 (structure **1**) on the rates of autoxidation of these complexes is remarkable (Table 2). Results are given here for studies in the MeOH/LiCl system. In all cases, the dioxygen dependence of the rates (averaged for 510 and 620–650 nm) obeys a saturation law and the data have been treated according to eqn. (9). The original rate constants are reported for a variety of conditions in Table 2. Table 5 summarizes the kinetic parameters calculated from the oxygen pressure dependence for the autoxidations.

Comparing rates for the MeOH/LiCl medium, the observed differences between the complexes are somewhat more dramatic than the previously reported values for APW [1]. In fact, the retardation that occurs upon replacing methyls by bulky groups at both the R^2 and R^3 positions is so great that the phenyl-*N*-benzyl substituted complex does not show appreciable autoxidation at the temperature at which the rates were measured for the other compounds, −25°C. Further, the rates reported for that complex were determined at room temperature, 20°C, some 45°

TABLE 5

Comparison of kinetic parameters for substituted iron(II) cyclidenes (R^1 = m-xyl)

Ligand	Solvent/base	T (°C)	K_b (torr^{-1})	k_a (torr^{-1} s^{-1})
Me,Me,m-xyl	MeCN/MIM	−16	0.046	2.1×10^{-4}
	MeOH/LiCl	−30	0.017	1.0×10^{-4}
		−29.5	0.018	4.3×10^{-4}
		−25	0.084	3.0×10^{-4}
Me,Bz,m-xyl	MeOH/LiCl	−25	0.012	2.3×10^{-5}
Ph,Me,m-xyl	MeOH/LiCl	−25	0.00075	3.1×10^{-6}
Ph,Bz,m-xyl	MeOH/LiCl	+20	0.0030	1.7×10^{-6}

higher. Using even the crudest extrapolation techniques, the rate constant k_a for $[Fe(Ph,Bz,m\text{-}xyl)Cl]^+$ autoxidation should lie between 5×10^{-8} and 10×10^{-8} $torr^{-1}$ s^{-1} at $-25°C$, representing an inhibition by a factor of between 10^3 and 10^4, when compared with the rate for $[Fe(Me,Me,m\text{-}xyl)Cl]^+$. The effect far exceeds that expected by replacing, for example, an electron-donating methyl group with a phenyl group (electronic effects are expected to parallel the iron(III)/iron(II) electrode potential [20]). The phenomenon may be another manifestation of the peculiar electron transfer kinetics associated with the O_2/O_2^- couple [21]. The fact that the effect of changing the two substituents ($\Delta E_{1/2} = +0.18$ V, Δrate $= 10^{3-4}\times$) far exceeds the sum of the effects of the two separate replacements ($\Delta E_{1/2} = +0.06$ and $+0.14$; Δrate $= 97\times$ and $13\times$), suggests that the effect may involve spatial, possibly steric, considerations rather than electronic relationships alone. R^2 more or less controls the bulk in the region around the smaller opening into the lacuna while R^3 clearly has a profound influence on the approaches to the larger opening into the cavity. It is fascinating to speculate that the overall effect of the bulky substituents might be to constrain the dioxygen molecule at locations too distant for orbital overlap and adiabatic electron transfer except when the O_2 molecule is well oriented to bind to the iron.

5. SUMMARY

The reaction products and kinetics of autoxidation of $[Fe^{II}(Me,Me,m\text{-}xyl)Cl]^+$ in the solvent systems MeOH/LiCl and MeCN/MIM represent two extremes. Even at low temperatures in MeOH/LiCl, with chloride serving as the axial ligand, a dioxygen adduct is not detectable and the only autoxidation products formed is high-spin $[Fe^{III}(Me,Me,m\text{-}xyl)OH]^{2+}$. In contrast, *N*-methyl imidazole is the axial ligand in MeCN/MIM, the dioxygen adduct is the dominant species, and the main autoxidation products are (peroxo)iron(III) species, that are similar to those previously detected for the APW solvent system [1]. More generally, in protic and wet systems where the axial ligand is chloride, no (peroxo)iron(III) species are formed, but the chloride ligand of $[Fe^{III}(Me,Me,m\text{-}xyl)Cl]^{2+}$ is replaced and hydroxo and μ-oxo derivatives are the main products. Kinetic behavior uniformly shows first-order dependence on the iron(II) complex and saturation behavior with respect to dioxygen pressure. However, the complexity of the interpretation increases as the O_2 binding ability of the reactant complex decreases. With the strong axial ligand and essentially aprotic medium of MeCN/MIM, the reaction dynamics are well modeled by a simple electron transfer between the iron(II) complex and dioxygen, in competition with dioxygen binding by the same complex. In contrast, in the highly polar, protic system MeOH/LiCl, the iron(II) complex gives little evidence of binding O_2 and the saturation kinetics derive from the combined effect of slight dioxygen binding and kinetic competency of the follow-up reaction of superoxide.

ACKNOWLEDGEMENTS

The financial support of the National Science Foundation, Grants number CHE-8822822 and CHE-9118455, and of the National Institutes of Health, Grant number RO1-GM10040, is gratefully acknowledged.

REFERENCES

1 A. Sauer-Masarwa, N. Herron, C.M. Fendrick and D.H. Busch, Inorg. Chem., 32 (1993) 1086.
2 L.D. Dickerson, A. Sauer-Masarwa, N. Herron, C.M. Fendrick and D.H. Busch, J. Am. Chem. Soc., in press.
3 D.H. Busch, Trasfus. Sangue, 33 (1988) 57.
4 N. Herron, L. Dickerson and D.H. Busch, J. Chem. Soc. Chem. Commun., (1983) 884.
5 (a) J. Weiss, Naturwissenschaften, 23 (1935) 64.
(b) P. George, J. Chem. Soc., (1954) 4349.
(c) G.S. Hammond and C.H. Wu, Adv. Chem. Ser., 77 (1968) 186.
(d) J.O. Alben, W.H. Fuchsman, C.A. Beaudreau and W.S. Caughey, Biochemistry, 7 (1968) 624.
(e) I.A. Cohen and W.S. Caughey, Biochemistry, 7 (1968) 636.
6 K.A. Goldsby, B.D. Beato and D.H. Busch, Inorg. Chem., 25 (1986) 2342.
7 N. Ye and D.H. Busch, Inorg. Chem., 30 (1991) 1819.
8 N. Herron, L.L. Zimmer, J.J. Grzybowski, D.J. Olszanski, S.C. Jackels, R.W. Callahan, J.H. Cameron, G.G. Cristoph and D.H. Busch, J. Am. Chem. Soc., 105 (1983) 6585.
9 W.J. Wallace, R.A. Houtchens, J.C. Maxwell and W.S. Caughey, J. Biol. Chem., 257 (1982) 4966.
J.A. Watkins, S. Kawanishi and W.S. Caughey, Biochem. Biophys. Res. Commun., 132 (1985) 742.
10 (a) P.R. Ortiz de Montellano, Cytochrome P450: Structure, Mechanism and Biochemistry, Plenum, New York, 1986.
(b) J.H. Dawson and K.S. Eble, Adv. Inorg. Bioinorg. Mech., 4 (1986) 1.
(c) R.E. White and M.J. Coon, Annu. Rev. Biochem., 49 (1980) 315.
11 (a) J. Stubbe and J.W. Kozarich, Chem. Rev., 87 (1987) 1107.
(b) M.C.R. Symons and R.L. Petersen, Biochim. Biophys. Acta, 535 (1978) 241.
(c) N. Bartlett and M.C.R. Symons, Biochim. Biophys. Acta, 744 (1982) 110.
(d) Z. Gasyna, FEBS Lett., 106 (1979) 213.
(e) R. Kappl, M. Hohn-Berlage, J. Huettermann, N. Bartlett and M.C.R. Symons, Biochim. Biophys. Acta, 827 (1985) 327.
(f) R. Davydov, R. Kappl, J. Huetterman and J.A. Peterson, FEBS Lett., 295 (1991) 113.
12 (a) M.H. Gubbelmann and A.F. Williams, Transition Metal Complexes. Structures and Spectra, Springer-Verlag, Berlin, Heidelberg, New York, Tokyo, 1983.
(b) E. McCandlish, A.R. Miksztal, M. Nappa, A.Q. Sprenger, J.S. Valentine, J.D. Strong and T.G. Spiro, J. Am. Chem. Soc., 102 (1980) 4268.
(c) J.N. Burstyn, J.A. Roe, A.R. Miksztal, B.A. Shaevitz, G. Lang and J.S. Valentine, J. Am. Chem. Soc., 110 (1988) 1382.
(d) S. Ahmad, J.D. McCallum, A.K. Shiemke, E.H. Appelman, T.M. Loehr and J. Sanders-Loehr, Inorg. Chem., 27 (1988) 2230.
(e) S. Fujii, H. Ohya-Nishiguchi and N. Hirota, Inorg. Chim. Acta, 175 (1990) 27.

(f) P.K.S. Tsang and D.T. Sawyer, Inorg. Chem., 29 (1990) 2848.
(g) C.H. Welborn, D. Dolphin and B.R. James, J. Am. Chem. Soc., 103 (1981) 2869.
(h) A. Shirazi and H.M. Goff, J. Am. Chem. Soc., 104 (1982) 6318.
13 P.A. Padolik, Ph.D. Thesis, The Ohio State University, 1989.
14 (a) K. Tajima, Kagaku to Kogyo (Tokyo), 44 (1991) 248.
(b) K. Tajima, Inorg. Chim. Acta, 169 (1990) 211.
(c) K. Tajima, Inorg. Chim. Acta, 163 (1989) 115.
(d) K. Tajima, M. Yoshino, K. Mikami, T. Edo, K. Ishizu and H. Ohya-Nishiguchi, Inorg. Chim. Acta, 172 (1990) 83.
(e) K. Tajima, M. Shigematsu, J. Jinno, K. Ishizu and H. Ohya-Nishiguchi, J. Chem. Soc. Chem. Commun., (1990) 144.
(f) K. Tajima, J. Jinno, K. Ishizu, H. Sakurai and H. Ohya-Nishiguchi, Inorg. Chem., 28 (1989) 709.
(g) K. Tajima, M. Shigematsu, J. Jinno, Y. Kawano, K. Mikamo, K. Ishizu and H. Ohya-Nishiguchi, Biochem. Biophys. Res. Commun., 166 (1990) 924.
(h) K. Tajima, M. Shigematsu, J. Jinno, K. Ishizu and H. Ohya-Nishiguchi, Stud. Surf. Sci. Catal., 66 (1991) 305.
15 (a) W.E. Blumberg and J. Peisach, in B. Chance, T. Yonetani and A.S. Mildvan (Eds.), Probes of Structure and Function of Macromolecules and Enzymes, Vol. II, Academic Press, New York, 1971, 215.
(b) S.C. Tang, S. Koch, G.C. Papaefthymiou, S. Foner, R.B. Frankel, J.A. Ibers and R.A. Holm, J. Am. Chem. Soc., 98 (1976) 2414.
16 (a) T. Ohtsuka, T. Ohya and M. Sato, Inorg. Chem., 24 (1985) 776.
(b) G.N. LaMar and J. Del Gaudio, in K.N. Raymond (Ed.), Bioinorganic Chemistry, Vol. II, 1977 p. 207.
17 (a) J. Peisach and W.E. Blumberg, in B. Chance, T. Yonetani and A.S. Mildvan (Eds.), Probes of Structure and Function of Macromolecules and Enzymes, Vol. II, Academic Press, New York, 1971, p. 231.
(b) A.X. Trautwein, E. Bill, E.L. Bominaar and H. Winkler, Struct. Bonding (Berlin), 78 (1991) 1.
18 J.S. Fritz, Acid–Base Titrations In Nonaqueous Solvents, Allyn and Bacon, Boston, 1973, p. 35.
19 D.M. Kurtz, Chem. Rev., 90 (1990) 585.
20 (a) D.H. Busch, D.G. Pillsbury, F.V. Lovecchio, A.M. Tait, Y. Hung, S. Jackels, M.C. Rakowski, W.P. Schammel and L.Y. Martin, in D.T. Sawyer (Ed.), Electrochemical Studies of Biological Systems, ACS Symp. Ser. 38, American Chemical Society, Washington, DC, 1977, p. 32.
(b) P.R. Warburton and D.H. Busch, in R.W. Hay (Ed.), Perspectives in Bioinorganic Chemistry, Vol. 2, in press.
21 K. Zahir, J.H. Espenson and A. Bakac, J. Am. Chem. Soc., 110 (1988) 5059.